

The Nature and Properties of a Repulsive Fermi Gas in the “Upper Branch”

Vijay B. Shenoy^{1*} and T.-L. Ho^{2†}

¹*Centre for Condensed Matter Theory, Indian Institute of Science, Bangalore 560 012, India and*

²*Department of Physics, Ohio State University, Columbus, OH 43210*

(Dated: May 2, 2022)

We generalize the Nozières-Schmitt-Rink (NSR) method to study the repulsive Fermi gas in the absence of molecule formation, i.e., in the so-called “upper branch”. We find that the system remains stable except close to resonance at sufficiently low temperatures. With increasing scattering length, the energy density of the system attains a maximum at a positive scattering length before resonance. This is shown to arise from Pauli blocking which causes the bound states of fermion pairs of different momenta to disappear at different scattering lengths. At the point of maximum energy, the compressibility of the system is substantially reduced, leading to a sizable uniform density core in a trapped gas. The change in spin susceptibility with increasing scattering length is moderate and does not indicate any magnetic instability. These features should also manifest in Fermi gases with unequal masses and/or spin populations.

PACS numbers: 03.75.Ss, 05.30.Fk, 67.85.-d, 67.85.Lm

Since the early days of quantum many-body theory, the Fermi gas with repulsive a short range interaction has been used as the primary example of a Fermi liquid ground state[1]. The discovery of BEC-BCS crossover[2], however, shows that the ground state of this system is a molecular condensate, and that the Fermi liquid state is metastable. In the last two years, after the ref. [3] suggested the evidence of Stoner ferromagnetism in these systems, there has been increasing interest in the nature of uncondensed Fermi gas (free of molecules) in the strongly interacting regime. Such systems have been referred to as the “upper branch” Fermi gas, while the molecular condensate is referred to as the “lower branch”.

Theoretical studies have found both ferromagnetic transition as well as the absence of it.[4] Though seldom emphasized, the upper branch Fermi gas in the strongly interacting regime has been studied by many experimental groups[5, 6] at higher temperatures with different densities and trap depths. The key features in atom loss and energy maximum reported in ref.[3] also appeared in these earlier experiments. A puzzling feature is the presence of a range of scattering length (a_s) where the energy derivative is negative ($\partial\mathcal{E}/\partial(-a_s^{-1}) < 0$) in apparent violation of the adiabatic relation of Tan[7]. Since the Fermi gas is unlikely to be ferromagnetic in the temperature regime of these earlier experiments, it leads to a natural and intriguing question on the nature of the repulsive gas in the strongly interacting regime.

The key obstacle in theoretical studies of the upper branch Fermi gas is to find a proper mathematical description of the “upper branch”. There is no precise formulation of it to the best of our knowledge. Fortunately, the meaning of upper branch is well defined in the high temperature regime, as the second virial coefficient b_2 is made up of a bound state contribution and an extended (or scattering) state contribution, $b_2 = b_2^{bd} + b_2^{sc}$. The upper branch corresponds to excluding the Hilbert space

of molecules by setting $b_2^{bd} = 0$. In addition, any description of the upper branch Fermi gas must also recover the well known results of Galitskii[1] in the weakly interacting limit, as the energies of the molecules are very far below the continuum and hence can be ignored.

Here we generalize the approach of NSR[8], which we call the excluded molecular pole approximation (EMPA), to study the upper branch Fermi gas. It amounts to excluding the Hilbert space of molecules in a Gaussian fluctuation theory[9], and obtaining thermodynamics within this truncated space. This approach recovers rigorously both the high temperature results and the results of Galitskii in the weak coupling limit. Applying this method to lower temperature and strongly interacting regime, we find the following: **(I)** On approaching the resonance from the repulsive side at a fixed temperature T , the energy density \mathcal{E} attains a maximum at a positive scattering length (a_{sm}) prior to resonance, as seen in experiments.[3, 6] Our theory also offers an explanation of the subsequent fall in the energy density with increasing a_s (violation of the adiabatic theorem of Tan). **(II)** The compressibility κ attains a minimum at a_{sm} (where \mathcal{E} is maximum). The small compressibility implies a core of almost uniform density at the centre of the trap. **(III)** The spin susceptibility χ attains a maximum at the location of the energy maximum, i. e., at a_{sm} ; it shows only a moderate variation over the entire range of a_s , without any divergence indicative of a magnetic instability.

EMPA for the Upper Branch Fermi Gas: Let us first recall that at low fugacity regime [10], the equation of state is $n(T, \mu) = n_o(T, \mu) + \partial\Delta P/\partial\mu$, where $n_o(T, \mu)$ is the density of an ideal gas, $\Delta P(T, \mu) = T(\sqrt{2}/\lambda)^3 z^2 b_2$ is the interaction contribution to the pressure, $\lambda = \sqrt{\frac{2\pi}{mT}}$ is the thermal wavelength, and $z = e^{\mu/T}$ is the fugacity (throughout, we set $\hbar = k_B = 1$), μ is the chemical potential. The second virial coefficient b_2 is made up of a bound state contribution b_2^{bd} and a scattering state

contribution b_2^{sc} , $b_2 = b_2^{bd} + b_2^{sc}$,

$$b_2^{bd} = e^{|E_b|/T}, \quad b_2^{sc} = \int_0^\infty \frac{d\omega}{\pi} \frac{d\eta}{d\omega} e^{-\omega/T}; \quad (1)$$

and $-|E_b| = -(ma_s^2)^{-1}$ is the energy of the bound state. The interaction contribution to equation of state $\Delta n(T, \mu) = n(T, \mu) - n_o(T, \mu)$ can therefore be written as $\Delta n = \Delta n^{bd} + \Delta n^{sc}$, where

$$\Delta n^\alpha(T, \mu) = \left(\frac{\sqrt{2}}{\lambda} \right)^3 b_2^\alpha T \frac{\partial z^2}{\partial \mu}, \quad \alpha = bd, \quad sc \quad (2)$$

Next we recall that in the NSR approach, the interaction contribution to the density $\Delta n(\mu, T) = n(T, \mu) - n_o(T, \mu)$ is

$$\Delta n(T, \mu) = -\frac{1}{\Omega} \sum_{\mathbf{q}} \int_{-\infty}^\infty \frac{d\omega}{\pi} n_B(\omega) \frac{\partial \arg M(\omega^+, \mathbf{q})}{\partial \mu}. \quad (3)$$

where $n_o(T, \mu) = 2 \sum_{\mathbf{k}} n_F(\xi_{\mathbf{k}})$, is the density of a two-component ideal Fermi gas, $n_F(\omega) = 1/(e^{\omega/T} + 1)$, $\xi_{\mathbf{k}} = \epsilon_{\mathbf{k}} - \mu$, $\epsilon_{\mathbf{k}} = \hbar^2 k^2/2m$, $n_B(\omega) = 1/(e^{\omega/T} - 1)$, and $M(\omega^+, \mathbf{q})$ is negative inverse of the two particle T-matrix in the medium, of the form

$$M(\omega^+, \mathbf{q}) = -\frac{1}{4\pi a_s} + L(\omega^+, \mathbf{q}) \quad (4)$$

$$L(\omega^+, \mathbf{q}) = \frac{1}{\Omega} \sum_{\mathbf{k}} \left(\frac{\gamma(\mathbf{k}; \mathbf{q})}{\omega^+ - \xi_{\frac{\mathbf{q}}{2} + \mathbf{k}} - \xi_{\frac{\mathbf{q}}{2} - \mathbf{k}}} + \frac{1}{2\epsilon_{\mathbf{k}}} \right), \quad (5)$$

$\gamma(\mathbf{k}; \mathbf{q}) = 1 - n_F(\xi_{\frac{\mathbf{q}}{2} + \mathbf{k}}) - n_F(\xi_{\frac{\mathbf{q}}{2} - \mathbf{k}})$ describes Pauli blocking of pair fluctuations, Ω is the volume. In the extreme dilute limit, $\gamma(\mathbf{k}; \mathbf{q})$ reduces to 1, and $-M^{-1}$ reduces to the inverse T-matrix of a two particle system, and the phase angle $\zeta(\omega, \mathbf{q}) \equiv \arg M(\omega^+, \mathbf{q})$ reduces to negative of the two-body phase shift $\eta(\omega - \omega(q))$, where $\omega(q) = q^2/4m - 2\mu$.

For a given \mathbf{q} , the value of $\zeta(\omega, \mathbf{q})$ depends on the location of branch cut and poles of $M^{-1}(\omega^+, \mathbf{q})$. It is clear from Eq.(4) and (5) that the branch cut is given by $\omega > \omega(q)$. Should $M^{-1}(\omega^+, \mathbf{q})$ have a pole, say at $\omega_b(q) < \omega(q)$, then we have

$$\omega > \omega(q), \quad \zeta(\omega, \mathbf{q}) = \tan^{-1} \left(\frac{\text{Im} L(\omega, \mathbf{q})}{-\frac{1}{4\pi a_s} + \text{Re} L(\omega, \mathbf{q})} \right), \quad (6)$$

$$\omega_b(q) < \omega < \omega(q), \quad \zeta(\omega, \mathbf{q}) = -\pi, \quad (7)$$

$$\omega < \omega_b(q), \quad \zeta(\omega, \mathbf{q}) = 0. \quad (8)$$

Otherwise, Eq.(7) and (8) are replaced by

$$\omega < \omega(q), \quad \zeta(\omega, \mathbf{q}) = 0. \quad (9)$$

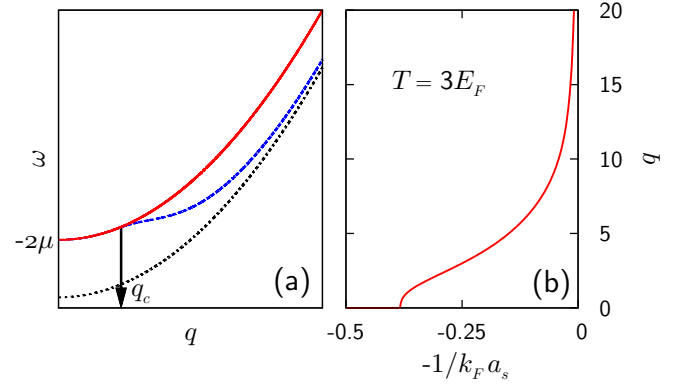


FIG. 1. (Color online) (a) Position of pole $\omega_b(q)$ in the (ω, q) -plane for a given a_s : The solid curve denotes the curve $\omega(q) = q^2/(4m) - 2\mu$. These pole position $\omega_b(q)$ is the solution of the equation $\text{Re} M(\omega^+, \mathbf{q}) = 0$ (see eqn. (4)), where Pauli blocking is described by $\gamma(\mathbf{k}; \mathbf{q})$. For $a_s > 0$, the matrix $M(\omega^+, \mathbf{q})$ of a two-body system will have a pole of energy $-|E_b|$ below $\omega(q)$, (dotted line). In a many body system, Pauli blocking will suppresses formation of molecular bound states. The suppression is strongest for pairs with total momentum $q = 0$ and is less strong for larger q . As a result the pole position changes to those indicated by the dashed blue curve. (b) The red curve is the critical scattering length $a_s^c(q)$ at $T = 3E_F$. (See (B) in *Summary of Results*). For a given a_s , a fermion pair with total momentum q (referred simply as “ q -pair”) can have a bound state only when $a_s < a_s^c(q)$, i.e., to the left of the red curve. As a_s increases, such that a_s crosses $a_s^c(q)$ from left to right, a q -pair will lose its bound state, and the energy of the scattering state of this pair will jump downward abruptly (see fig. 4).

Eq.(3) can then be written as $\Delta n(T, \mu) = \Delta n^{bd}(T, \mu) + \Delta n^{sc}(T, \mu)$,

$$\Delta n^{bd}(T, \mu) = -\frac{1}{\Omega} \sum_{\mathbf{q}} n_B(\omega_b(q)) \frac{\partial \omega_b(q)}{\partial \mu} \quad (10)$$

$$\Delta n^{sc}(T, \mu) = -\frac{1}{\Omega} \sum_{\mathbf{q}} \int_{\omega(q)}^\infty \frac{d\omega}{\pi} n_B(\omega) \frac{\partial \zeta(\omega, \mathbf{q})}{\partial \mu}. \quad (11)$$

That we use the same superscript in Eq.(10) and (11) as in the high temperature case is because they reduce to Eq.(2) in the low fugacity regime. Thus, by continuity, the extension of the upper branch Fermi gas to lower temperature is to *exclude the contribution from the molecular bound pole term (Eq.(10)) from $\Delta n(T, \mu)$* . Hence the name EMPA. The equation of state within EMPA is then

$$n(T, \mu) = n_o(T, \mu) + \Delta n^{sc}(T, \mu). \quad (12)$$

Considering a system with fixed density n (which defines E_F and the associated k_F in the discussion below) and inverting the relation $n = n(T, \mu)$ to obtain $\mu = \mu(n, T)$, one can obtain all thermodynamic potentials as a function of n and T . [11] It is also straightforward to describe spin polarized states in the upper branch by including a magnetic field h .

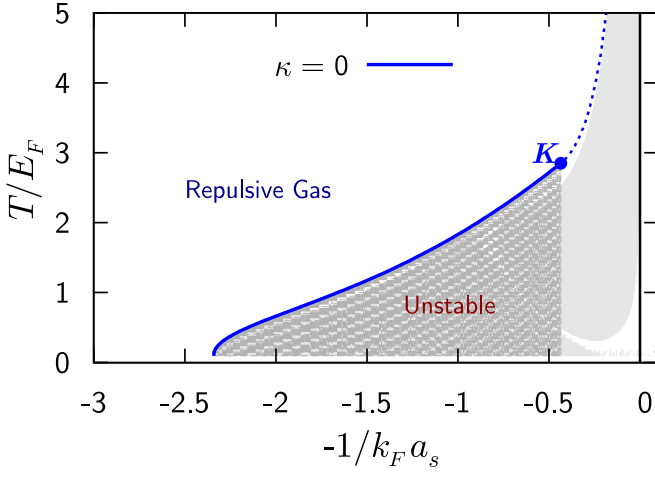


FIG. 2. (Color online) Upper branch “phase diagram”. The point \mathbf{K} corresponds to $(-1/k_F a_s = -0.435, T = 2.85E_F)$. The solid blue line ending at \mathbf{K} is a locus of states with a vanishing compressibility. The dashed curve starting at \mathbf{K} shows a_{sm} (see text). The region hatched in dark grey is mechanically unstable. Tan’s adiabatic theorem is violated in the region shaded in light grey.

Note that Eq.(12) involves only integrating over the area $\omega > \omega(q)$ (i. e., above the solid curve in Fig. 1(a)) with an integrand given by explicitly Eq.(6). There is no need to obtain the pole structure as far as evaluating Eq.(12) is concerned. There is, however, a close connection between the interaction energy of scattering state and the presence of a pole. Understanding the distribution of poles in the ω - q plane is, therefore, essential for the elucidation of the results to be presented below.

(A) *Phase diagram*: Fig. 2 displays the “phase diagram” of upper branch Fermi gas. All regions except the region in dark grey are stable ($\kappa, \chi > 0$). The solid line that ends at \mathbf{K} is the boundary of vanishing compressibility $\kappa = 0$. The dashed line above \mathbf{K} describes a_{sm} where the energy attains a maximum at a fixed temperature. Across this line, μ , κ , χ , and energy density \mathcal{E} are continuous but their slope undergoes sharp changes. These discontinuous slopes, however, may disappear if beyond Gaussian fluctuations are included. Crossing the solid line below the point \mathbf{K} , the quantities μ , P , κ , χ , and \mathcal{E} undergo discontinuous changes; the system is mechanically unstable. The white and light grey regions correspond to regimes with $\partial\mathcal{E}/\partial(-a_s^{-1}) > 0$ and $\partial\mathcal{E}/\partial(-a_s^{-1}) < 0$ respectively. In the light grey region, Tan’s adiabatic theorem is not applicable (see below).

(B) *Energy density \mathcal{E}* : Fig. 3(a) shows the behavior of energy density \mathcal{E} as a function of $k_F a_s$ at $T = 3T_F$. It exhibits a maximum at $k_F a_{sm} = 2.61$, (which falls on the dashed line in Fig. 2 at this temperature). Such maximum feature is consistent with the early observation by Salomon’s group[6] at high temperatures, as well as in ref.[3] at lower temperatures. The maximum be-

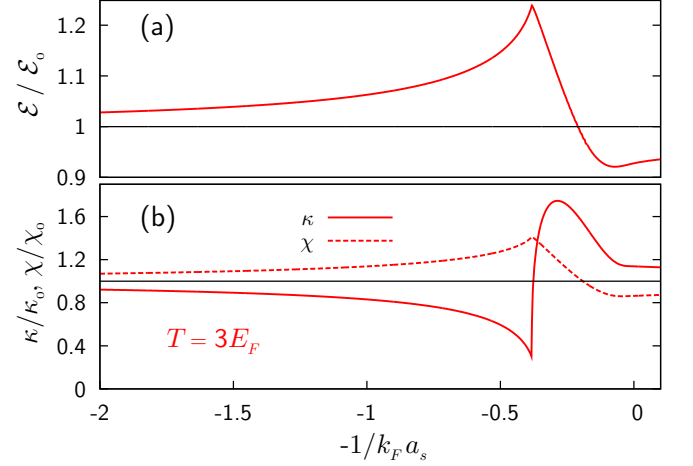


FIG. 3. (Color online) (a) Energy density (\mathcal{E}) and (b) compressibility (κ) and susceptibility (χ) as a function of the scattering length at $T = 3E_F$. All quantities are measured in units of their respective values of the non-interacting gas (indicated by the subscript o) at the same temperature.

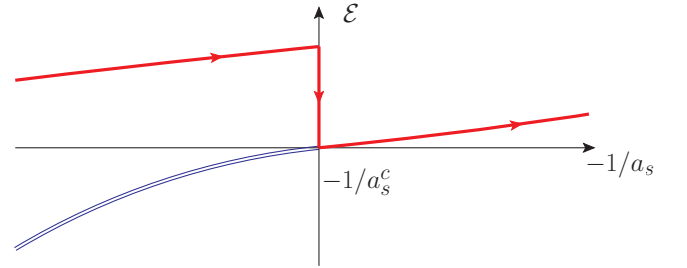


FIG. 4. (Color online) The discontinuous change of the energy of the scattering state (solid line) of a two body system up on the disappearance of the molecular bound state (double line). [10] Similar phenomena occur in a q -dependent fashion in the many body setting.

havior implies that there is a region of $k_F a_s$ (the light grey region in Fig. 2) where the the adiabatic theorem, $\partial\mathcal{E}/\partial(-a_s^{-1}) > 0$ is violated. The resolution is that the relation between $\partial\mathcal{E}/\partial(-a_s^{-1})$ of the scattering state and the contact density is ill-defined at the scattering length where a molecular bound state disappears.

This is best seen in the two-body case (see Fig. 4), where the energy of the scattering state of a fermion pair with total momentum \mathbf{q} (referred to as “ \mathbf{q} -pairs”) jumps suddenly downward when of a_s passes a critical value ($(a_s^c)^{-1} = 0$ in this case) at which the molecular bound state on the side $a_s < (a_s^c)^{-1}$ disappears. In the many-body case, due to Pauli blocking, $(\gamma(\mathbf{k}; \mathbf{q}) \neq 1)$, different \mathbf{q} -pairs will form bound states at different critical scattering length $a_s^c(q)$ (which is the lowest value of a_s such that the equation $\text{Re}M(\omega, \mathbf{q}) = 0$ has a solution). Since Pauli blocking effect is strongest for the $\mathbf{q} = 0$ molecular bound state (Fig. 1(a)), and is less significant as

q increases, $(a_s^c(q))^{-1}$ is largest at $q = 0$ and decreases monotonically as q increases. The behavior of a_s^c is shown in Fig. 1(b), and $a_{sm} \equiv a_s^c(q = 0)$.

That $\partial\mathcal{E}/\partial(-a_s^{-1}) < 0$ for upper branch Fermi gas sufficiently close to resonance is now clear. As a_s passes through $a_s^c(q)$ from below, the molecular bound state of a q -pair disappears because of Pauli blocking. Up on this disappearance, the energy of the scattering states of this pair suddenly jumps down, thereby causing the energy to decrease. As a_s continues to increase, fermions pairs with successively higher total momentum q lose their bound states, inducing a successive downward jump in the energies of the scattering states of these pairs, and hence a negative derivative $\partial\mathcal{E}/\partial(-a_s^{-1}) < 0$. Note that since a_{sm} is determined only by Pauli blocking, it should be a universal function T and n i.e., $k_F a_{sm} = f(T/E_F)$, where f is a dimensionless function (dashed line in Fig. 2).

Our explanation above might lead one to think that the energy decreasing process will cease when no more q -pairs lose their bound states, which occurs at $a_s = \infty$. What actually happens, however, is that the minimum of \mathcal{E} as a_s increases beyond a_{sm} (which signifies the ceasing of energy decrease) occurs at a scattering length prior to resonance. The reason is that in order to have an energy decrease caused by the scattering state of a q -pair, this pair state has to be occupied. At lower temperatures, the probability of occupation of such pair states is low especially for those pairs with high q , thereby causing the energy decrease to cease at an $(a_s)_{min}$ prior to resonance. At T increases, $((a_s)_{min})^{-1}$ approaches 0.

(D) *Compressibility κ* : As a_s increases, a repulsive Fermi gas is expected to become less compressible. For temperatures above that of point **K** in Fig. 2, κ attains a minimum at $a_s = a_{sm}$ (see Fig. 3(b)). Our calculation shows, for temperatures lower than that of **K**, $\kappa \rightarrow 0$ as one approaches the solid line (Fig. 2) from the left. The system behaves like a hard core Fermi gas with a core size close to inter-particle spacing. There is, however, an important difference between a hard core Fermi gas with core size equal $a_s \approx k_F^{-1}$ and the actual atomic Fermi gas. In the former case, the effective range is also of order k_F , whereas the effective range in atomic gases is much less than inter-particle spacing, independent of the value of a_s . The diminished compressibility has a dramatic effect on the density profile. This leads to clouds with little variation of density at the centre, an effect the becomes more pronounced at lower temperatures (see Fig. 5).

(C) *Spin susceptibility χ* : Fig. 3(b) also shows the spin susceptibility χ at $T = 3T_F$. Note that χ changes by at most 40 percent for the entire $k_F a_s$ range, and only moderately in the experimentally relevant range $0.5 < k_F a_s < 2$. We do not see a diverging susceptibility indicative of a magnetic transition.

Although our discussions focused on the equal-mass spin- $\frac{1}{2}$ Fermi gas, the properties enumerated arise mainly from Pauli blocking. These features should, therefore, be

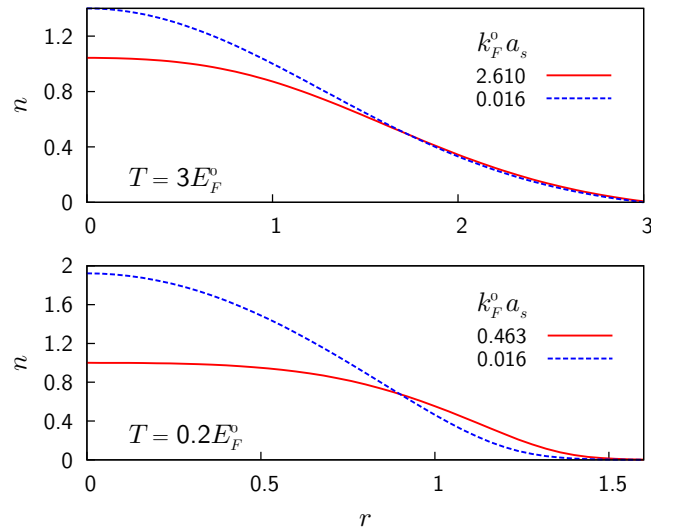


FIG. 5. (Color online) Comparison of densities of strongly interacting and weakly interacting gases in a spherical trap. E_F^0 corresponds to the density at the trap centre. For each temperature, the number of atoms in both the strong and weak cases is the same. A “flat-top” density profile is evident in the strong case, and becomes more pronounced at lower temperatures. The radius r is in units of $\sqrt{\frac{2E_F^0}{m\omega_t}}$ (ω_t - trap frequency).

generic to other upper branch Fermi gases, such as those with unequal masses or unequal spin populations.

VBS thanks DAE (SRC-grant) and DST (Ramanujan-grant) for support. T-LH is supported by NSF Grant DMR-0907366 and by DARPA under the Army Research Office Grant Nos. W911NF-07-1-0464, W911NF0710576, and the Tsinghua University Initiative Scientific Research Program. This paper was completed during the INT Workshop on Fermions From Cold Atom to Neutron Star in May 2011.

* shenoy@physics.iisc.ernet.in

† jasontlho@gmail.com

- [1] V. M. Galitskii, Sov. Phys.-JETP, **7**, 104 (1958).
- [2] C. A. Regal, M. Greiner, and D. S. Jin, Phys. Rev. Lett. **92**, 040403 (2004)
- [3] Gyu-Boong Jo, Ye-Ryoung Lee, Jae-Hoon Choi, Caleb A. Christensen, Tony H. Kim, Joseph H. Thywissen, David E. Pritchard, Wolfgang Ketterle, Science, Vol. 325, 1521-1524 (2009).
- [4] T. Sogo and H. Yabu, Phys. Rev. A **66**, 043611 (2002). T. Maruyana and G. Bertsch, Phys. Rev. A **73**, 013610 (2002). R. A. Duine and A. H. MacDonald, Phys. Rev. Lett. **95**, 230403 (2005). S. Pilati, G. Bertainia, S. Giorgini, and M. Troyer, Phys. Rev. Lett. **105**, 030405 (2010). S.-Y. Chang, M. Randeria, and N. Trivedi, Proc. Nat. Acad. Sci., **108**, 51 (2011). S.Q. Zhou, D.M. Ceperley and S. Zhang, arXiv:1103.3534.

- Chia-Chen Chang, Shiwei Zhang, David M. Ceperley Phys. Rev. A **82**, 061603(R) (2010), L. J. Le Blanc, J. H. Thywissen, A. A. Burkov, and A. Paramekanti, Phys. Rev. A **80**, 013607 (2009). G.J.Conduit and B. Simons, Phys.Rev.Lett. **103**,200403 (2009) H. Heiselberg, arXiv:1012.4569v1. H. . Zhai, Phys.Rev.A **80** 051605(R) 2009 X. Cui and H. Zhai, *ibid.*, **81**, 041602R (2010). D. Pekker et al., arXiv:1005.2366. D. Pekker, M. Babadi, R. Sensarma, N. Zinner, L. Pollet, M. W. Zwierlein, and E. Demler, PRL **106** 050402 (2011).
- [5] K.Dieckmann, C.A. Stan, S.Gupta, Z. Hadzibabic, C.H. Schunck and W. Ketterle, Phys.Rev.Lett. **89**, 203201 (2002), C.A. Regal, M.Greiner and D.S. Jin, Phys.Rev.Lett. **92**, 083201 (2004). S.Jochim, M.Bartenstein, A.Altmeter, G.Hendl, C.Chin, J.Hecker Denschlag and R.Grimm, Phys.Rev.Lett. **91**, 240042 (2003); see also S.Jochim, dissertation, Bose-Einstein Condensation of Molecules, University of Innsbruck, 2004.
- [6] T.Bourdel, J.Cubizolles, L.Khaykovich, K.M.F. Magalhães, S.J.J.M.F. Kokkelmans, G.V.Shlyapnikov and C. Salomon, Phys.Rev.Lett. **91**, 020402 (2003).
- [7] S. Tan, Ann. Phys. **323**, 2952 (2008); **323**, 2971 (2008) and **323**, 2987 (2008).
- [8] P. Nozières and S. Schmitt-Rink, J. Low Temp. Phys. **59**, 195 (1985).
- [9] C. A. R. Sà de Melo, M. Randeria, and J. R. Engelbrecht, Phys. Rev. Lett. **71**,3202 (1993).
- [10] T.-L. Ho and E. J. Mueller, Phys. Rev. Lett. **92**, 160404 (2004) and references therein.
- [11] From the density, pressure P , compressibility κ , entropy density s , and total energy \mathcal{E} can be calculated as $P(T, \mu) = \int_{-\infty}^{\mu} d\mu' n(T, \mu')$, $\kappa(T, \mu) = \partial n(T, \mu) / \partial \mu$, $s(T, \mu) = \partial P / \partial T$, $\mathcal{E} = Ts - P + \mu n$. Spin density and susceptibility can be similarly calculated by introducing a magnetic field h .